Research Article **Open Access**

Jose Rubén Morones-Ibarra*, Armando Enriquez-Perez-Gavilan, Abraham Israel Hernández Rodriguez, Francisco Vicente Flores-Baez, Nallaly Berenice Mata-Carrizalez, and Enrique Valbuena Ordoñez

Chiral symmetry restoration and the critical end point in QCD

https://doi.org/10.1515/phys-2017-0130
Received June 20, 2017; accepted November 10, 2017

Abstract: In a system of quark matter we study the chiral phase transition, the behavior of the chiral and quark number susceptibility and the CEP at finite temperature and chemical potential. This is done within the framework of two-flavor Nambu and Jona-Lasinio model. We have calculated the chiral quark condensate and the quark number density and, with this, we have found the phase transition type. With these quantities we have determined the phase diagram for QCD and the CEP.

Keywords: chiral phase transition, critical end point, dynamical mass, critical behavior, dynamical chiral symmetry breaking

PACS: 05.70.Fh, 11.30.Rd, 12.38.Aw, 12.39.x

1 Introduction

One of the main purposes of the experiments of relativistic heavy-ion collisions at Large Hadron Collider (LHC) and Relativistic Heavy Ion Collider (RHIC) is the observation of restoration of chiral symmetry at finite temperature and at finite density [1, 2]. This has led to an increasing interest in the study of strongly interacting matter subject to extreme conditions of temperature and density [3, 4]. In this work we study the structure of the chiral phase diagram of Quantum Chromodynamics (QCD) in order to determine the critical end point (CEP) and to describe the behavior of the quark condensate and the chiral and quark number susceptibilities.

Strongly interacting particles is one of the contemporary research topics in theoretical and experimental physics, due in part to the possibility of conducting experiments in order to test the theoretical results obtained from different models [5, 6]. Several experiments currently in progress at the RHIC and LHC [7, 8] stimulate the interest in this subject.

QCD is generally accepted to be the fundamental theory that describes strong interactions [9, 10]. In the limit of massless quarks, the chiral symmetry determines the characteristics of the phase diagram of QCD [11, 12]. One of the most important features of QCD is the spontaneous chiral symmetry breaking (SCSB) [13, 14]. Through the SCSB we analyze the behavior of the quark condensate as a function of the temperature (T) and the chemical potential (μ) in order to determine the phase diagram in the T-μ plane.

The most powerful tool to study the QCD phase diagram at finite temperature is the lattice QCD simulation [15, 16]. With this technique it is possible to analyze the QCD phase diagram of strongly interacting matter under extreme conditions of density and temperature [6, 11]. One of the limitations of this method is the sign problem, that is, the Pauli blocking, due to the fact that the lattice simulation fails to apply for finite chemical potential [13].

The usual way to study the (partial) restoration of chiral symmetry in QCD is considering a system of quarks described by an effective theory model [17]. In this paper we follow the Nambu and Jona-lasinio (NJL) model applied to quarks as degrees of freedom at finite temperature and at finite chemical potential.

The study of phase transition in QCD requires the definition of order parameters. These order parameters are related with the two main characteristics of the QCD: the chiral symmetry breaking and confinement. The order parameter related to the chiral symmetry is the quark condensate, where $\langle \bar{q}q \rangle = 0$ for the chiral symmetric phase and $\langle \bar{q}q \rangle \neq 0$ for the phase where the chiral symmetry has been

***Corresponding Author: Jose Rubén Morones-Ibarra:** Facultad de Ciencias Físico-Matemáticas, Universidad Autónoma de Nuevo León, Pedro de Alba S/N, San Nicolás de los Garza, Nuevo León 66451, México, E-mail: jose.moronesib@uanl.edu.mx
Armando Enriquez-Perez-Gavilan, Abraham Israel Hernández Rodriguez, Francisco Vicente Flores-Baez, Nallaly Berenice Mata-Carrizalez, Enrique Valbuena Ordoñez: Facultad de Ciencias Físico-Matemáticas, Universidad Autónoma de Nuevo León, Pedro de Alba S/N, San Nicolás de los Garza, Nuevo León 66451, México

broken. With regard to confinement, we find two different phases: the hadronic matter phase, which is observed at low temperatures and densities, and the quark-gluon plasma state, which occurs at high temperatures and/or densities [13, 16].

It is necessary to understand the properties of the QCD vacuum in order to study these phases [18, 19]. The QCD ground state is characterized by the quark condensate [20], which is the consequence of the SCSB.

In the present work we study the chiral phase, particularly the CEP, which is the point where a change in the nature of the phase transition occurs. Following the critical line in the QCD phase diagram from high to low temperature, at first a second order phase transition is present at the chiral limit (crossover occurs instead for a bare mass $m > 0$). We find the point (CEP) in the critical line, from which a first-order phase transition occurs.

We investigate the quark number susceptibility in order to locate the CEP in a system of quarks at finite temperature and chemical potential. Once the position of the CEP is found, there is enough information to determine the phase transition type present under specific conditions of T and μ [21, 22].

The most important contribution of this work is the determination of the location of the CEP in the T-μ plane through the use of the scalar (chiral) susceptibility and the quark number susceptibility. The criterion to judge the phase transition type is determined through the analysis of the scalar and quark number susceptibilities.

A discontinuity in the effective quark mass (as a function of T and μ) at the phase transition (the critical line in the QCD phase diagram) indicates that a first order phase transition takes place. On the other hand, a continuous behavior of the effective mass at the critical line of the phase diagram indicates that a second order phase transition (in the chiral limit) or a crossover (for $m > 0$) occurs. The values of T and μ in the phase diagram where a crossover, a first order phase transition or a second order phase transition takes place, can be obtained by studying the divergence in the susceptibilities [23].

2 Formalism

In 1961, the NJL model was originally developed for the study of interacting nucleons [17]. This is a pioneer chiral model for massless fermions where these particles acquire mass through the spontaneous chiral symmetry breaking. Initially, it consisted of an isospin-doublet built of nucleons, and later it was extended to describe the interaction between quarks as degrees of freedom [24]. In this work, we apply the NJL model to study the chiral dynamical behavior of a system consisting of two kind of light quarks at finite temperature and chemical potential. Our starting point for this investigation is the Lagrangian density [25], which is invariant under global chiral $SU_L(2) \otimes SU_R(2)$ rotations at the massless limit, and is given by

$$\mathcal{L}_{NJL} = \bar{\psi}(i\partial\!\!\!/ - \hat{m})\psi + g\left[(\bar{\psi}\psi)^2 + (\bar{\psi}i\gamma_5\tau^a\psi)^2\right] \tag{2.1}$$

where the column vector $\psi = (u, d)$ represents the quark fields with N_f flavors and N_c colors, $\hat{m}$ is the bare quark mass matrix $\hat{m} = \mathrm{diag}(m_u, m_d)$, g is the effective coupling constant and τ^a are the Pauli matrices. We set $m = m_u = m_d$ in this paper.

According to the Fierz transformation, which formulates how the direct and exchange terms are related to each other, the part of the Lagrangian, equation (2.1), which contains the four-point interaction terms ($\mathcal{L}_{IF}$) is equivalent to [6, 20]

$$\begin{aligned}\mathcal{L}_{IF} = \frac{g}{8N_c}[&2(\bar{\psi}\psi)^2 + 2(\bar{\psi}i\gamma_5\tau^a\psi)^2 - 2(\bar{\psi}\tau^a\psi)^2 \\ &- 2(\bar{\psi}i\gamma_5\psi)^2 - 4(\bar{\psi}\gamma_\mu\psi)^2 - 4(\bar{\psi}i\gamma_\mu\gamma_5\psi)^2 \\ &+ (\bar{\psi}\sigma^{\mu\nu}\psi)^2 - (\bar{\psi}\sigma^{\mu\nu}\tau^a\psi)^2]\end{aligned} \tag{2.2}$$

and it leads to the following Lagrangian [26]

$$\mathcal{L} = \bar{\psi}(i\partial\!\!\!/ - m)\psi + \hat{\mu}\bar{\psi}\gamma_0\psi + G_s(\bar{\psi}\psi)^2 - G_v(\bar{\psi}\gamma_\mu\psi)^2 \tag{2.3}$$

where $G_s = \left(1 + \frac{1}{4N_c}\right) g$ and $G_v = g/2N_c$ are the scalar and vector couplings, respectively and $\hat{\mu}$ is the chemical potential matrix $\hat{\mu} = \mathrm{diag}(\mu_u, \mu_d)$. We consider here only the scalar-scalar channel. A term has been introduced in the Hamiltonian density ($\mathcal{H}$) connected via a Legendre transformation to Lagrangian density, equation (2.1), $\mathcal{H} \to \mathcal{H} - \hat{\mu}\mathcal{N}$, where $\mathcal{N} = \bar{\psi}\gamma_0\psi = \psi^\dagger\psi$ is the quark number density operator. Only the simple physical case $\mu = \mu_u = \mu_d$ is considered in this paper.

The NJL model is non-renormalizable due to the four-point interaction and therefore a certain regularization scheme is required to isolate divergences. We work in the 3D cut-off scheme, introducing the cut-off scale, a usual parameter in effective non-renormalizable models [27].

Using the mean-field approximation [3]

$$(\bar{\psi}\Gamma\psi)^2 \longrightarrow 2\langle\bar{\psi}\Gamma\psi\rangle\bar{\psi}\Gamma\psi - \langle\bar{\psi}\Gamma\psi\rangle^2 \tag{2.4}$$

where Γ can be any one of the 4×4 matrices such as I, γ_5, γ_μ, $\gamma_5\gamma_\mu$, we we take $\langle\bar{\psi}\psi\rangle$ and $\langle\bar{\psi}\gamma_0\psi\rangle$ as mean fields in the vacuum at finite temperature and density. After this, the Lagrangian in equation (2.3), is simplified to

$$\mathcal{L}_{MF} = \bar{\psi}(i\partial\!\!\!/ - M + \mu_r\gamma_0)\psi - \frac{(M-m)^2}{4G_s} + \frac{(\mu-\mu_r)^2}{4G_v} \tag{2.5}$$

where M is the effective quark mass defined as

$$M = m - 2G_s\langle\bar{\psi}\psi\rangle \tag{2.6}$$

and μ_r is the renormalized quark chemical potential

$$\mu_r = \mu - 2G_v\langle\psi^\dagger\psi\rangle \tag{2.7}$$

The equation (2.6) is the well-known NJL gap equation for the dynamical fermion mass M which is related to the quark condensate. The scalar density may be expressed in terms of the quark propagator as

$$\langle\bar{\psi}\psi\rangle = -i\mathrm{Tr}S(0) = -i\mathrm{Tr}\int\frac{d^4p}{(2\pi)^4}\frac{\not{p}+M}{p^2-M^2} \tag{2.8}$$

Similarly, the quark number density is given by

$$\langle\psi^\dagger\psi\rangle = -i\mathrm{Tr}\int\frac{d^4p}{(2\pi)^4}\frac{\gamma_0(\not{p}+M)}{p^2-M^2} \tag{2.9}$$

where the symbol Tr stands for the trace over color-, flavor- and Dirac-indices. In order to describe the system at non vanishing temperature T and chemical potential μ, momentum integrals are carried out in the imaginary time formalism

$$i\int\frac{d^4p}{(2\pi)^4}f(p_0,\vec{p}) \longrightarrow -T\sum_{n=-\infty}^{+\infty}\int\frac{d^3\vec{p}}{(2\pi)^3}f(i\omega_n+\mu_r,\vec{p}) \tag{2.10}$$

The quark propagator is then defined at discrete imaginary energies $i\omega_n + \mu_r$, where $\omega_n = (2n+1)\pi T$, are the Matsubara frequencies for fermions. After performing the Matsubara sums, integrating over angular components in equations (2.8) and (2.9), and substituting into equations (2.6) and (2.7), respectively, we obtain

$$M(T,\mu) = m + \frac{2G_sN_fN_c}{\pi^2}\int_0^\Lambda p^2\,dp\frac{M}{E}\left(1-f^+-f^-\right) \tag{2.11}$$

$$\mu_r(T,\mu) = \mu + \frac{G_vN_fN_c}{\pi^2}\int_0^\Lambda p^2\,dp\left(f^+-f^-\right) \tag{2.12}$$

with

$$f^\pm(T,\mu_r) = \frac{1}{e^{(E\pm\mu_r)/T}+1} \tag{2.13}$$

where $E = \sqrt{\vec{p}^{\,2}+M^2}$ is the quark energy, $f^{(\pm)}$ are the Fermi occupation number of quarks (+) and anti-quark (-) and Λ is a momentum cut-off.

The scalar and the quark number susceptibilities are of particular interest in this work. It is known that variations of conserved charges are susceptible evidences of the thermal state of the medium as well as its critical behavior. The scalar susceptibility $\chi_s = \frac{\partial M}{\partial m}$, is generally defined as the response of the constituent quark mass to changes of the bare quark mass [22]. It is related to the order parameter $\langle\bar{q}q\rangle$ by

$$\chi_s = \frac{1}{1-\frac{2G_sN_cN_f}{\pi^2}\frac{\partial}{\partial M}\int_0^\Lambda p^2\,dp\frac{M}{E}\left[1-f^{(+)}-f^{(-)}\right]} \tag{2.14}$$

In order to measure the first order response of quark number density to a change of the quark chemical potential, we consider the quark number susceptibility χ_q [28, 29], which is defined as

$$\chi_q = \frac{\partial\langle\psi^\dagger\psi\rangle}{\partial\mu_r} \tag{2.15}$$

From this information and the divergences present in the susceptibilities, we determine the location and characteristics of the chiral phase transition for a system of quarks with parameters T and μ. Then, we obtain the phase diagram for the constituent quark mass M, as well as the critical behavior and the position of the CEP.

3 Results

The results for the effective quark mass as a function of temperature and chemical potential, from the gap equation (2.6) were obtained for $m = 0$ and $m = 3.5$ MeV. These particular values were chosen because of their relevance in the expected results. The chiral limit is considered for $m = 0$ MeV, which leads to the total restoration of the chiral symmetry and to a second order phase transition for $T > T_{CEP}$ at the critical line in the phase diagram. In contrast, for a finite quark bare mass, the results yield a partial restoration of the chiral symmetry and to a crossover between phases for $T > T_{CEP}$ at the critical line. This can be observed in Figure 1, where only for a finite m, the effective mass, M, is greater than 0 above the critical temperature. The value for $m = 3.5$ MeV was selected in order to represent the light u and d quarks behavior, since the approximation $m = m_u = m_d$ was considered in this paper.

As commented in Section 2, since the NJL model is perturbatively nonrenormalizable, a regularization scheme must be selected in order to regulate the divergent quantities. Regularization must take into account the physically expected properties and maintain the symmetries considered in the model. For the NJL model, from the minimization of the total energy, the gap equation must be obtained, and the appearance of a Goldstone boson, due to symmetry requirements, needs to be considered [20]. The scheme selected in this study was the 3D cut-off scheme (through the use of imaginary time formalism). Within this scheme,

Table 1: Results obtained for different bare masses (data shown in [GeV])

m	M	T_c	μ_c	T_{CEP}	μ_{CEP}
0.0000	0.3129	0.1899	0.3380	0.0715	0.2877
0.0035	0.3228	0.2034	0.3436	0.0469	0.3212

the NJL model requires 2 parameters to be determined: the coupling strength, G_s, and the momentum cut-off value, Λ. These parameters are ordinarily set by selecting physical quantities (namely, the constant pion decay f_π and the quark condensate density, $\langle\bar{\psi}\psi\rangle$, whose values have been measured experimentally) in the QCD vacuum. By solving the gap equation, considering the values $f_\pi = 93$ MeV and $\langle\bar{\psi}\psi\rangle = -(250\text{MeV})^3$, the parameters G_s and Λ can be obtained. For the 3D cut-off scheme, the parameter values considered were $\Lambda = 0.653$ [GeV] and $G_s\Lambda^2 = 2.14$ [20].

From the results obtained for the effective quark mass in each case, the chiral (scalar) susceptibility and quark number susceptibility were also computed. Finally, from these results, the quark phase diagram, critical temperature (T_c), critical chemical potential (μ_c) and the CEP were obtained for the two values considered for the bare masses. The numerical solutions were obtained using Matlab 2015a©. The results obtained are shown in Table 1.

In the upper panel of Figure 1, we plot the phase diagram of QCD for the two-flavor NJL model in the T-μ plane for the cases of $m = 0$ and $m = 3.5$ MeV. For the chiral limit, the critical temperature is found to be $T_c \approx 190$ MeV and the critical chemical potential $\mu_c \approx 338$ MeV, and for $m = 3.5$ MeV, $T_c \approx 203$ MeV and $\mu_c \approx 343$ MeV. Figure 1 also displays the location of the tri-critical point (TCP), at $T_{TCP} = 71.5$ MeV and $\mu_{TCP} = 287.7$ MeV, and the CEP, at $T_{CEP} = 46.9$ MeV and $\mu_{CEP} = 321.2$ MeV. The behavior of the effective quark mass as a function of temperature at $\mu = 0$ for $m = 0$ and $m = 3.5$ MeV is presented in the lower panel of Figure 1. The effective quark mass presents small variations for the lower values of temperature, with an increasing rate of change as the temperature increases, until the effective mass value drops to 0 (at T_c in the chiral limit and asymptotically for $m > 0$)

As indicated in Section 2, the chiral susceptibility χ_s is the response of the effective quark mass to the changes of the bare mass. The results for χ_s are displayed in Figure 2, where it is observed that χ_s is divergent only in the TCP (in the chiral limit) or the CEP (for massive quarks), and is finite elsewhere. In the upper panel (chiral limit), it is found that for $T < T_{TCP}$, χ_s is discontinuous and, for $T > T_{TCP}$, χ_s is continuous at the transition chemical potential, indicating the existence of a first-order phase transition for

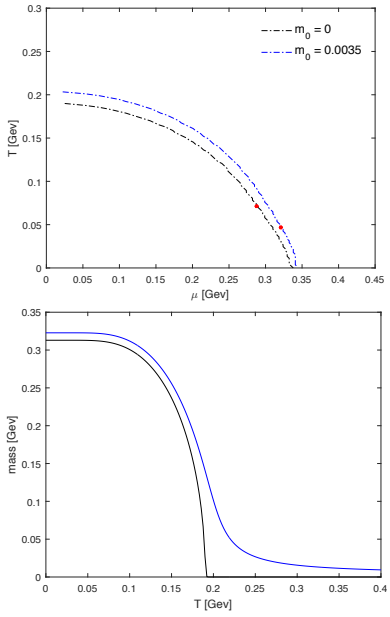

Figure 1: The upper figure shows the T-μ phase diagram for the cases of chiral limit and $m = 3.5$ MeV. The red points indicate the TCP and the CEP respectively. The lower figure represents the effective quark mass vs temperature at $\mu = 0$ with $m = 0$ and for the case of nonzero $m = 3.5$ MeV.

$T < T_{TCP}$ and the existence of a second-order phase transition for $T > T_{TCP}$. In the lower panel, it is found that for $T > T_{CEP}$, χ_s is a smooth continuous function at the transition chemical potential, indicating the existence of a crossover region for $T > T_{CEP}$. The CEP reported in this paper was obtained from the analysis of the chiral susceptibility.

In Figure 3 (upper panel) the quark number susceptibility is presented as a function of the chemical potential for $m = 0$ and $T > T_{CEP}$ (91.6 MeV), $T = T_{CEP}$ (71.5 MeV), and $T < T_{CEP}$ (51.4 MeV). Also Figure 3 (lower panel) shows the quark number susceptibility as a function of the chemical potential for $m = 3.5$ MeV and $T > T_{CEP}$ (67 MeV), $T = T_{CEP}$ (46.9 MeV), and $T < T_{CEP}$ (26.8 MeV).

4 Discussion

Chiral and quark number susceptibilities are important phenomenological observables which hold information about the changes in the quark chemical potential [30, 31]. In this work we have solved the gap equation for the quark propagator and we have used the chiral susceptibility to analyze the solution of the gap equation. With this tool we have classified the order of the phase transitions. In the $T - \mu$ plane, we observe that for $\mu = 0$, there is a second order chiral phase transition at a temperature $T = T_c$. This

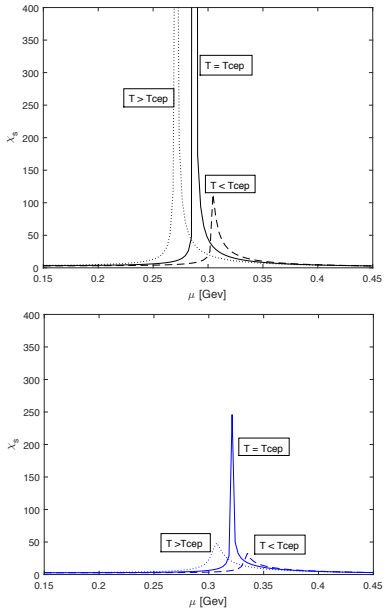

Figure 2: Scalar susceptibility χ_s as a function of μ. Upper panel: in the chiral limit for three different temperatures around to the TCP; Lower panel: with m = 3.5 MeV for three different temperatures around to the CEP.

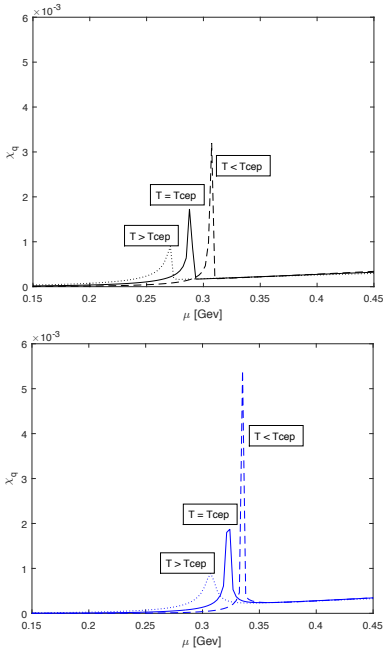

Figure 3: Upper panel: Quark number susceptibility χ_q as a function of μ in the chiral limit for different temperatures around to the TCP. Lower panel: Quark number susceptibility χ_q as a function of μ with m = 3.5 MeV for different temperatures around to the CEP.

second order phase transition is consistent with the lattice QCD simulations and several QCD models [15, 16]. On the other hand, for $T = 0$, we observe that the chiral symmetry restoration, which occurs at a finite chemical potential $\mu = \mu_c$, is a transition of first order. This result is also consistent with that obtained in different models of QCD [23, 32, 33].

Both the scalar susceptibility and quark susceptibility exhibit a divergence at the CEP. The CEP was obtained through the analysis of the behavior of these susceptibilities. We have found that the CEP over the critical line that separates both types of transitions is located at ≈ (46.9,321.2) MeV, as shown in Table 1.

We also observe that, as the quark bare mass is increased, the values of μ_c and T_c are shifted to higher values, while the CEP is shifted to higher values of μ and lower values of T.

Finally, we compare the results obtained with that of previous works.

The work presented by Y Lu et al. [6] also follows the NJL model and study the behavior of the susceptibilities in order to determine the TCP (at the chiral limit) and the CEP (for the massive quark). In [6], for the massless quark, the values $T_{TCP} \approx 73$ MeV and $\mu_{TCP} \approx 300$ MeV are reported. These results show resemblance to the ones teported in Table 1. For the massive quark, the values $T_{CEP} \approx 32$ MeV and $\mu_{TCP} \approx 347$ MeV.

The difference with the results obtained for a massive quark lies mainly in the value selected for the quark bare mass. We selected a value of $m = 3.5$ MeV, while in [6] the value $m = 5.5$ MeV was used in the analysis. We observe, however, that the CEP reported in [6] is shifted to higher values of μ and lower values of T with respect to the values we report, which is consistent with the behavior observed in the results we have obtained. Another difference present when both studies are compared is the values selected for the momentum cut-off and the coupling strength. We have taken the values reported by [20], while in [6] the parameter values are obtained from [34]. In [35], for instance, different values are reported for m = 5.0 MeV.

The work presented by Y Zhao, L Chang, W Yuan and Y-X Liu [29] follows as well the NJL model and the 3D cut-off scheme; this work studies the phase transition of the quark with respect to μ, setting $T = 0$. In this work, the critical chemical potential is reported to be $\mu_c = 368$ MeV for the chiral limit and $\mu_c = 385$ MeV for $m = 5.6$ MeV.

For the massive quark, the differences in the μ_c with respect to the results we report are, in part, due to the value selected for the bare mass. Since the quark bare mass considered in [29] is greater than the one we have chosen, and the value of μ_c reported in [29] is shifted to a higher value with respect to the one we acquired, the results show consistency. In [29], the parameter values are reported to be Λ = 588 MeV and $G_S\Lambda^2 = 2.44$. This explains the difference observed in μ_c for the massless quark.

We observe that the values for the parameters in the NJL model depend on the value chosen for the quark bare mass; therefore considering these parameters as constants is an approximation useful only for small variations in m. Future work in this subject will include the study of the variation of the coupling strength and the momentum cut-off with respect to the quark bare mass.

5 Conclusions

By using the NJL model in the SU(2) version at finite temperature and chemical potential we have studied the QCD chiral phase diagram in the $T - \mu$ plane. We have found a second order chiral phase transition (at the chiral limit) and a crossover (for $m > 0$), which persists for increasing values of the chemical potential, up to a CEP, after which the chiral transition becomes of first order. The values of CEP are shown above in Table 1.

Acknowledgement: A. Hernandez gratefully acknowledges scholarship support from the National Council for Science and Technology (CONACYT) under contract No. 290817-UANL. Also F. Flores acknowledges SNI (Conacyt).

References

[1] Arsene I. *et al.*, Quark-gluon plasma and color glass condensate at RHIC? The perspective from the BRAHMS experiment, Nucl. Phys. A, 2005, 757, 1-27
[2] Martínez G., Advances in Quark Gluon Plasma, arXiv:1304.1452, 2013
[3] Vogl U., Weise W., The Nambu and Jona-Lasinio model: Its implications for Hadrons and Nuclei, Prog. Part. Nucl. Phys., 1991, 27, 195-272
[4] Evans N. *et al.*, On the QCD Ground State at High Density, Nucl. Phys. B, 2000, 581, 391-408
[5] Buballa M., NJL-model analysis of dense quark matter, Phys. Rept., 2004, 407, 205-376
[6] Lu Y. *et al.*, Critical behaviors near the (tri-)critical end point of QCD within the NJL model, Eur. Phys. J. C, 2015, 75, 495-501
[7] Adams J. *et al.*, Experimental and theoretical challenges in the search for the quark-gluon plasma: The STAR Collaboration's critical assessment of the evidence from RHIC collisions, Nucl. Phys. A, 2005, 757, 102-183
[8] Lacey R. *et al.*, Has the QCD Critical Point Been Signaled by Observations at the BNL Relativistic Heavy Ion Collider?, Phys. Rev. Lett., 2007, 98, 092301
[9] Birrell J., Rafelski J., Quark-gluon plasma as the possible source of cosmological dark radiation, Phys. Lett. B, 2015, 741, 77-81
[10] Engel G., Giusti L., Lottini S., Sommer R., Chiral symmetry breaking in QCD with two light flavors, Phys. Rev. Lett., 2015, 114, 112001
[11] Carlomagno J., Gómez Dumm D., Scoccola N., Inhomogeneous phases in nonlocal chiral quark models, Phys. Rev. D, 2015, 92, 056007
[12] Luo X., Spontaneous chiral-symmetry breaking of lattice QCD with massless dynamical quarks, Sci. China G, 2007, 50, 6-14
[13] Chelabi K. *et al.*, Realization of chiral symmetry breaking and restoration in holographic QCD, arXiv:1511.02721, 2015
[14] Alexandru A., Horváth I., Chiral polarization scale of QCD vacuum and spontaneous chiral symmetry breaking, J. Phys. Conf. Ser., 2013, 432, 012034
[15] Karsch F., Deconfinement and Chiral Symmetry Restoration, arXiv:hep-lat/9903031, 1998
[16] Makiyama T. *et al.*, Phase structure of two-color QCD at real and imaginary chemical potentials: Lattice simulations and model analyses, Phys. Rev. D, 2016, 93, 014505
[17] Nambu Y., Jona-Lasinio G., Dynamical Model of Elementary Particles Based on an Analogy with Superconductivity, Phys. Rev., 1961, 122, 345-358
[18] Reinhardt H., Weigel H., Vacuum nature of the QCD condensates, Phys. Rev. D, 2012, 85, 074029
[19] Wetterich C., Connection between chiral symmetry restoration and deconfinement, Phys. Rev. D, 2002, 66, 056003
[20] Klevansky S., Nambu–Jona-Lasinio model of quantum chromodynamics, Rev. Mod. Phys., 1992, 64, 649-708
[21] Zhao Y. *et al.*, Relation between chiral susceptibility and solutions of gap equation in Nambu–Jona-Lasinio model, arXiv:hep-ph/0610358, 2006
[22] Du Y-L. *et al.*, Susceptibilities and critical exponents within the Nambu-Jona-Lasinio model, Int. J. Mod. Phys. A, 2015, 30, 1550199
[23] Anh N., Tam D., Phase transitions in a chiral model of nuclear matter, Phys. Rev. C, 2011, 84, 064326
[24] Koch V. *et al.*, A chirally invariant fermionic field theory for nuclear matter, Phys. Lett. B, 1987, 185, 1-5
[25] Kohyama H., Kimura D., Inagaki T., Regularization dependence on phase diagram in Nambu–Jona-Lasinio model, Nucl. Phys. B, 2015, 896, 682-715
[26] Coelho J. *et al.*, Quarks stars in SU(2) Nambu-Jona-Lasinio model with vector coupling, Nucl. Phys. Proc. Suppl., 2010, 199, 325-328
[27] Kneur J-L., Pinto M., Ramos R., Thermodynamic and phase structure of the two-flavor Nambu-Jona-Lasinio model beyond large N_c, Phys. Rev. C, 2010, 81, 065205
[28] Aarts G. *et al.*, Electrical conductivity and charge diffusion QCD from the lattice, JHEP, 2015, 02, 186
[29] Zhao Y. *et al.*, Chiral susceptibility and chiral phase transition in Nambu-Jona-Lasinio model, Eur. Phys. J. C, 2008, 56,483-492
[30] Ghosh S. *et al.*, Quark number susceptibility: Revisited with fluctuation-dissipation theorem in mean field theories, Phys. Rev. D, 2014, 90, 054030
[31] Cui Z-F. *et al.*, Progress in vacuum susceptibilities and their applications to the chiral phase transition of QCD, Annals Phys., 2015, 358, 172-205
[32] Jiang Y. *et al.*, Quark number susceptibility around the chiral critical end point, Chin. Phys. Lett., 2015, 32, 021201
[33] Carlomagno J., Gómez D., Scoccola N., Deconfinement and chiral restoration in nonlocal SU(3) chiral quark, Phys. Rev. D, 2013, 88, 074034
[34] Hatsuda T., Kunihiro T., QCD phenomenology based on a chiral effective Lagrangian, Phys. Rep., 1994, 247, 221-369
[35] Bernard V., Jaffe R., Meißner U., Flavor mixing via dynamical chiral symmetry breaking, Phys. Lett. B, 1987, 198, 92-98